Methylmercury Alters the Activities of Hsp90 Client Proteins, Prostaglandin E Synthase/p23 (PGES/23) and nNOS

Samuel Caito[1], Heng Zeng[2], Judy L. Aschner[3], Michael Aschner[1,2,3,4]*

1 Department of Molecular Pharmacology, Albert Einstein College of Medicine, Bronx, New York, United States of America, 2 Department of Pediatrics, Vanderbilt University School of Medicine, Nashville, Tennessee, United States of America, 3 Department of Pediatrics and Obstetrics & Gynecology and Women's Health, Albert Einstein College of Medicine of Yeshiva University and Children's Hospital at Montefiore, Bronx, New York, United States of America, 4 The Kennedy Center, Albert Einstein College of Medicine, Bronx, New York, United States of America

Abstract

Methylmercury (MeHg) is a persistent pollutant with known neurotoxic effects. We have previously shown that astrocytes accumulate MeHg and play a prominent role in mediating MeHg toxicity in the central nervous system (CNS) by altering glutamate signaling, generating oxidative stress, depleting glutathione (GSH) and initiating lipid peroxidation. Interestingly, all of these pathways can be regulated by the constitutively expressed, 90-kDa heat shock protein, Hsp90. As Hsp90 function is regulated by oxidative stress, we hypothesized that MeHg disrupts Hsp90-client protein functions. Astrocytes were treated with MeHg and expression of Hsp90, as well as the abundance of complexes of Hsp90-neuronal nitric oxide synthase (nNOS) and Hsp90-prostaglandin E synthase/p23 (PGES/p23) were assessed. MeHg exposure decreased Hsp90 protein expression following 12 h of treatment while shorter exposures had no effect on Hsp90 protein expression. Interestingly, following 1 or 6 h of MeHg exposure, Hsp90 binding to PGES/p23 or nNOS was significantly increased, resulting in increased prostaglandin E_2 (PGE_2) synthesis from MeHg-treated astrocytes. These effects were attenuated by the Hsp90 antagonist, geldanmycin. NOS activity was increased following MeHg treatment while cGMP formation was decreased. This was accompanied by an increase in $\cdot O_2^-$ and H_2O_2 levels, suggesting that MeHg uncouples NO formation from NO-dependent signaling and increases oxidative stress. Altogether, our data demonstrates that Hsp90 interactions with client proteins are increased following MeHg exposure, but over time Hsp90 levels decline, contributing to oxidative stress and MeHg-dependent excitotoxicity.

Introduction

Methylmercury (MeHg) is a potent neurotoxicant. Studies from mass poisonings in Japan and Iraq, as well as the examination of seafood-rich diets of the Seychelles and Faroe Islands, have illustrated the effects of MeHg on human populations [1,2]. MeHg causes focal lesions, such as loss of cerebellar granular cells and occipital lobe damage, and during extreme poisonings can lead to ataxia, numbness of extremities, muscle weakness, vision and hearing problems, and paralysis in adults [3]. Developmental exposure to MeHg leads to microcephaly and inhibition of neuronal migration, distortion of cortical layers, cerebellar abnormalities, alterations in neurotransmitter systems and alterations in glial cells [3]. Astrocytes, in particular, are highly susceptible to the toxic effects of MeHg. Astrocytes are a preferred cellular site for MeHg accumulation and it has been shown that MeHg-induced neuronal dysfunction is secondary to astrocytic disturbances [4,5,6,7]. MeHg inhibits astrocytic uptake systems for cysteine and cystine, glutamate and aspartate, compromising the cell's redox potential, attenuating glutathione (GSH) content,

increasing extracellular glutamate concentrations and sensitizing neurons for excitotoxic injury [8,9,10,11,12].

MeHg is a potent inducer of oxidative stress through the generation of reactive oxygen species (ROS). H_2O_2, superoxide anion (O_2-) and nitric oxide (NO) levels are increased in cultured neurons, astrocytes and in rodent brains following MeHg exposure [13,14]. Putative mechanisms of MeHg-induced free radical generation include inhibition of mitochondrial electron transport chain complexes II and III, alterations in antioxidant enzyme function, and activation of nitric oxide synthase (NOS) [15,16,17]. Additionally, as an electrophile, MeHg reacts readily with thiol and selenol groups on proteins as well with GSH, leading to inhibition of enzymes and alteration of protein structure. This has been described for both glutathione peroxidase and thioredoxin antioxidant enzymes [18,19]. Altering antioxidant activity and depletion of GSH leads to a more oxidized environment and further generation of ROS, creating a vicious cycle. It is unknown how MeHg affects the 90-kDa heat shock protein (Hsp90), an important regulator of cellular redox status.

Hsp90 is one of the most abundant proteins in eukaryotic cells, constituting 1–2% of total intracellular protein [20]. It is constitutively and ubiquitously expressed and is the most abundant molecular chaperone protein. Chaperones help to achieve and maintain the conformational status of cellular proteins and enzyme complexes by influencing higher order protein structure. Hsp90 protects its client proteins from degradation, which is in contrast to other chaperones, such as Hsp70, which tend to direct misfolded proteins to degradation [21]. Hsp90 is involved in the conformational regulation of key proteins in multiple signaling pathways, including kinases, phosphatases, steroid hormone receptors, nitric oxide synthases and prostaglandin E synthase/p23 (PGES/p23) [22,23,24,25], many of which are involved in MeHg-induced neurotoxicity. Hsp90 contains two key reactive cysteine residues, which along with the stabilizing molybdate, regulates the redox status of client proteins by assisting in the formation and breakage of disulfide bridges [26]. Oxidizing conditions impair the chaperone activity and lead to cleavage of Hsp90, which can cause client protein degradation and cell death [26,27,28]. Therefore, we hypothesized that MeHg inhibits Hsp90-client protein interactions and consequently disrupts Hsp90 client protein functions. We tested this hypothesis by measuring Hsp90 expression and protein-protein interactions between Hsp90 and its client proteins, PGES/p23 and nNOS in astrocytes following MeHg exposure. Additionally, we examined prostaglandin E_2 (PGE$_2$) and NO levels as measures of PGES/p23 and nNOS enzymatic functions, respectively.

Materials and Methods

Reagents

Unless otherwise stated, all biochemical reagents used in this study were purchased from Sigma Chemicals (St. Louis, MO, USA).

Primary cell culture and treatments

Primary astrocytes were isolated from cortical tissue of postnatal day-1 neonatal Sprague-Dawley rats, as previously described [29,30]. After dissociation, centrifugation and resuspension, the mixed glial cell culture was maintained in 225 cm^2 tissue culture treated flasks fed with minimum essential medium (MEM; Invitrogen, Carlsbad, CA), supplemented with 10% heat-inactivated horse serum (Invitrogen), 100 U/ml penicillin and 100 μg/ml streptomycin. The cultures were maintained in a humidified incubator at 37°C of 5% CO_2. The media were changed twice a week. After 2 weeks in culture, when cells reached ∼95% confluence, microglia and astrocytes were separated by gentle shaking for 20 min at room temperature. Using this protocol, our lab has achieved ≥95% purity of the isolated astrocytes, as verified by immunostaining for glial fibrillary acidic protein (GFAP) [29,30]. Equal densities of astrocytes were plated in poly-L-lysine coated plates (BD Biocoat, San Jose, CA). Cells were treated with MeHgCl (ICN Biomedicals, Costa Mesa, CA) in a concentration-dependent (1, 5, or 10 μM) or time-dependent (10 min to 24 h) manner using concentrations that have been shown not to significantly alter cytotoxicity [30,31]. To examine the effects of COX-1/2 inhibition, Hsp90 antagonism, and glutathione (GSH) depletion, astrocytes were pretreated with indomethacin (0.01 mM x 15 min), geldanamycin. (1 μM x 30 min), and a GSH synthesis inhibitor, buthionine sulfoximine (BSO; 100 mM x 24 h), respectively, before MeHg treatment. To stimulate nNOS expression from astrocytes, cells were treated with LPS (1 μg/ml x 18–24 h) and IFNγ (100 u/ml x 18–24 h) prior to MeHg treatment.

Western Blot Analysis

Following MeHg treatments, cells were scraped and collected in radioimmunoprecipitation assay (RIPA) buffer with protease inhibitor cocktail on ice. Protein concentrations of the cell lysates were determined using the bicinchoninic acid (BCA) assay (Pierce, Rockford, IL). Twenty μg of protein were loaded onto a 10% SDS-PAGE acrylamide gel. Proteins were electroblotted onto polyvinylidene difluoride membranes, blocked with 0.1% Tween PBS with 5% nonfat milk, and western blots were performed with the primary antibodies anti-Hsp90a/b (sc-13119, Santa Cruz Biotechnology, Santa Cruz, CA), anti-PGES/p23 (Cayman Chemical Co, Ann Arbor, MI, or GeneTex, Inc., San Antonio. TX), anti-nNOS, and anti-iNOS (BD Biosciences, San Jose, CA or MyBioSource, Inc. San Diego, CA), and β-actin (A5316, Sigma). Proteins were visualized by species-appropriate secondary antibodies labeled with horseradish peroxidase (Santa Cruz Biotechnology) and chemiluminescent substrate (ECL; Amersham Pharmacia Biotech).

Immunofluorescence

Primary astrocytes were grown on 8-well chamber slides (1×104 cells/well), treated with MeHg (1 or 5 μM), and then fixed in 4% paraformaldehyde for 10 min. The cells were then permeabilized for 10 min in 0.3% Triton X-100 in PBS, and blocked for 1 h using 10% normal goat serum in PBS. Samples were incubated with antibodies specific for Hsp90 in a humidified chamber overnight. The primary antibody was detected with an anti-mouse secondary antibody. Nuclei were stained with SYTOX Green (Life Technologies, Grand Island, NY). The coverslips were mounted onto the slides using VectaShield (Vector Laboratories, Burlingame, CA, USA) and viewed under a Nikon Ellipse 80i microscope (Nikon, Tokyo, Japan).

Co-immunoprecipitation Assay

To examine protein-protein interactions with Hsp90, 500 μg of protein were precleared with pansorbin and then incubated for 6 h at 4°C with either anti-nNOS or anti-Hsp90 antibodies (1 μg/mg total cell protein). Immune complexes were precipitated by overnight incubation at 4°C with protein G-sepharose. The next morning, beads were then washed in lysis buffer and pelleted to remove all unbound protein. The immunoprecipitated samples were heated at 80°C for 15 min in Laemmli loading buffer, and proteins were resolved by SDS-PAGE as described above.

PGE2 and cGMP Quantification

Levels of PGE$_2$ release into cell culture media and cGMP from protein extracts of astrocytes treated with MeHg were measured using PGE$_2$ and cGMP enzyme immune assays (EIA; Cayman Chemical, Ann Arbor, MI), respectively, according to the manufacturer's instructions. The developed chromogen absorbance was measured at 405 nm using a VMAX 96-well plate spectrophotometer (Molecular Devices).

Estimation of RONS Formation

To quantify the effect of MeHg on astrocyte reactive oxygen and nitrogen species, three fluorescent dyes were applied to the cells. For the detection of NO, 20 μM 4,5-diaminofluorescein diacetate (DAF2DA; Molecular Probes, Grand Island, NY) was applied to cells following MeHg treatment (30 min with 10 μM MeHg). In the presence of •NO and oxygen, the non-fluorescent DAF2 is converted to the green fluorescent triazole, DAF2T. After addition of DAF2DA, fluorescence images were taken at an excitation wave length of 488 nm and emission wave length of

515 nm. To assess $\cdot O_2^-$ production, cells were loaded with hydroethidium (10 µM), and treated with 10 mM MeHg for 20 min. Images from the hydroethidium and DAF2DA staining were obtained by confocal microscopy (LSM510; Zeiss 63X water immersion objective, Carl Zeiss MicroImaging, Inc). The resultant confocal data were quantitatively analyzed using the Zeiss LSM software (Carl Zeiss MicroImaging, Inc). To assess H_2O_2 production astrocytes were loaded for 30 min with 50 µM $2',7'$-dichlorodihydrofluorescein diacetate (H_2DCFDA, Life Technologies) before treatment with MeHg (5, 10, 20 µM) in HEPES buffer, and the fluorescence intensity was monitored using a multiwell fluorescence plate reader, as previously described [32].

Statistical Analysis

All results were expressed as means ± standard errors with a minimum of three independent experiments. One-way analysis of variance (ANOVA) and two-way ANOVA followed by Bonferroni's *post hoc* test were performed using Prism 4 (Graphpad Software Inc., San Diego, CA). Values of P<0.05 were considered statistically significant.

Results

MeHg alters Hsp90 protein expression

As MeHg is a strong electrophile and Hsp90 is abundant in cysteine residues, we first examined the direct effect of MeHg on Hsp90 protein levels. Neonatal rat primary astrocytes were treated for 1 h with 1 or 5 µM MeHg. Cells were then stained for Hsp90 by immunofluorescence. Nuclei were stained with Sytox dye. Treatment with MeHg caused a concentration-dependent decrease in Hsp90 immunoflorescence (Figure 1A). Similarly, Western blot analysis of whole-cell extracts from astrocytes treated with 1 µM MeHg showed significant loss of Hsp90 protein levels following 12 and 24 h of exposure (Figure 1B). Hsp90 protein expression was not significantly different from control for exposures under 12 h.

MeHg increases PGE$_2$ production by altering the binding of Hsp90 to PGES/p23

Previously, we reported that MeHg causes time- and concentration-dependent release of arachidonic acid (AA) from astrocytes, associated with increased expression of phospholipase A$_2$ (cPLA$_2$) mRNA and protein [33]. This effect was fully reversed by treatment with the specific cPLA$_2$ inhibitor, AACOCF$_3$, suggesting a direct effect of MeHg on cPLA$_2$ [33]. Here we examined a downstream effect of AA release, namely the formation of PGE$_2$. PGE$_2$ levels were first measured in cell culture media from astrocytes treated with 1, 5, or 10 µM MeHg for 3 h. Treatment with 1 µM MeHg had no significant effect, but both 5 and 10 µM MeHg treatments increased PGE$_2$ release when compared to untreated cells (Figure 2A). Analogous dose-dependent effects of MeHg were seen following 1 and 6 hrs exposures (data not shown). We next measured PGE$_2$ release from astrocytes treated with 10 µM MeHg over the time course of 10 min to 360 min (Figure 2B). We have previously shown that MeHg increases AA release from astrocytes over a similar time course [33]. MeHg significantly increased PGE$_2$ levels at all time points examined, with the highest release at 360 min (Figure 2B).

PGE$_2$ is formed by the actions of cyclooxygenase-1 (COX-1) and PGE$_2$ synthase (PGES/p23). PGES/p23 requires glutathione (GSH) for optimal activity and is a Hsp90 cofactor [34]. PGE$_2$ release was measured from astrocytes treated with 10 µM MeHg for 3 hours in the presence of COX-1/2 inhibitor indomethacin (Indo, 0.01 mM), Hsp90 antagonist geldanamycin (GA, 1 µM), or
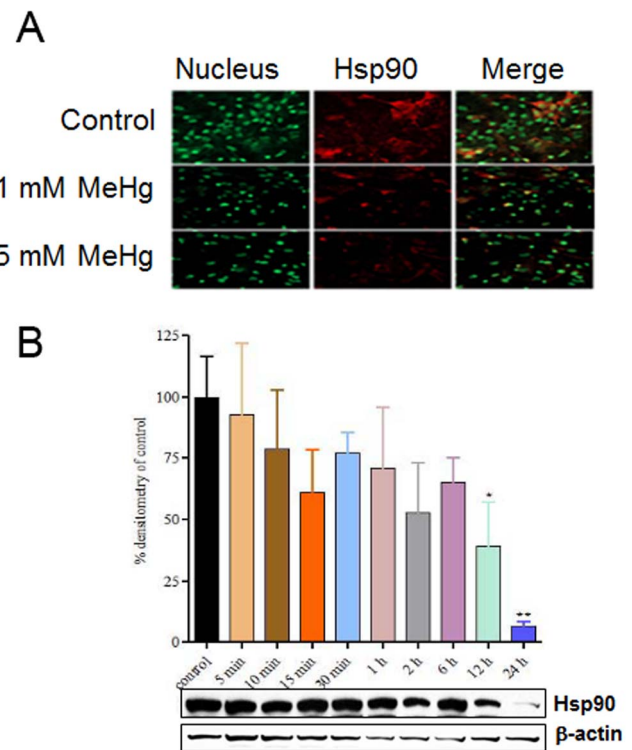

Figure 1. MeHg alters Hsp90 protein expression. (A) Neonatal rat primary astrocytes were treated for 1 h with 1 or 5 µM MeHg. Cells were fixed with 4% paraformaldehyde and used for immunostaining with an anti-Hsp90 monoclonal antibody (red) and Sytox (green) nuclear dye. (B) Astrocytes were treated with 1 µM MeHg for 5, 10, 15, 30 min, 1, 2, 6, 12, or 24 h. Whole cell extracts were used for immunoblot analysis for Hsp90. Results are the mean ± SEM from 4-6 separate astrocyte preparations. *p<0.05, **p<0.01 vs. control.
doi:10.1371/journal.pone.0098161.g001

GSH depletion agent, buthionine sulfoximine (BSO, 100 mM) (Figure 2C).

Inhibition of COX-1/2 by indomethacin abolished MeHg-induced PGE$_2$ release (Figure 2C). Likewise, BSO inhibited MeHg-stimulated PGE$_2$ production. GA significantly decreased the amount of PGE$_2$ released from the astrocytes upon MeHg treatment (Figure 2C), suggesting that Hsp90 function is important for MeHg-induced PGE$_2$ synthesis and release.

As PGES/p23 is known to interact with Hsp90 we examined whether MeHg alters this interaction to promote PGE$_2$ synthesis. Astrocytes were treated with 10 µM MeHg for 1 or 6 h in the presence or absence of an 18–24 h pre-treatment with LPS (1 µg/ml)/IFNγ (100 u/ml). LPS/INFγ activates astrocytes to upregulate glial fibrillary acidic protein (GFAP), iNOS and nNOS, as well as release proinflammatory, neurotrophic and neurotoxic mediators [35,36]. After MeHg treatment, Hsp90 was immunoprecipitated from whole-cell protein extracts and levels of PGES/p23 were examined by immunoblot. Following 1 h MeHg treatment there was increased binding of Hsp90 and PGES/p23 when astrocytes were activated with LPS/IFNγ (Figure 3). The reverse experiment (immunoprecipitation with anti-PGES/p23 antibody and immunoblotting with anti-Hsp90 antibody) also confirmed markedly enhanced Hsp90/PGES binding following 6 h MeHg exposure (data not shown).
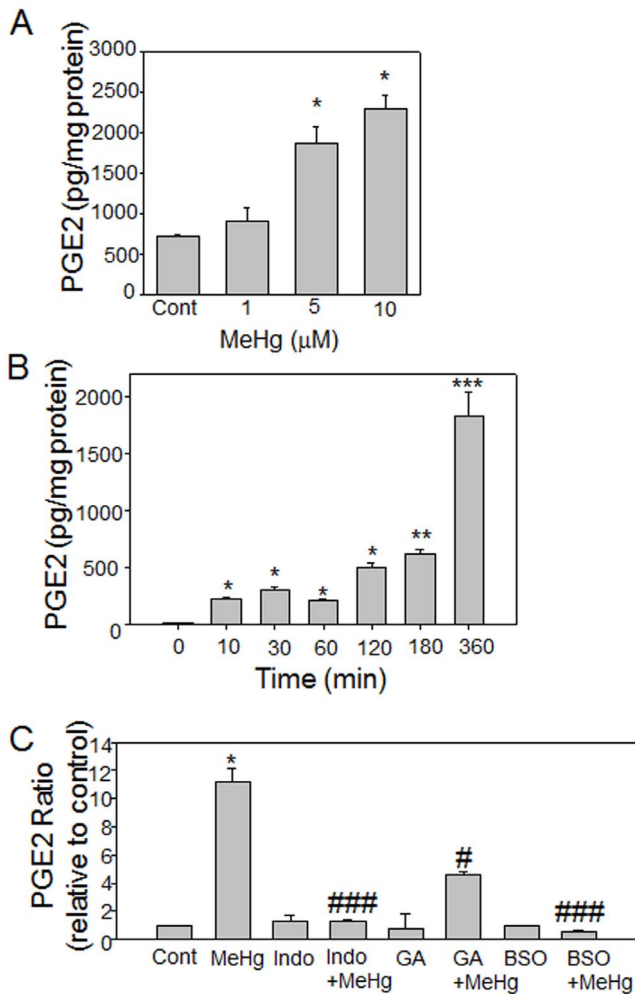
Figure 2. MeHg increases PGE$_2$ levels. Astrocytes were treated with (A) 1, 5 and 10 μM MeHg for 3 h or (B) 10 μM MeHg for 10, 20, 60, 120, 180, or 360 min. PGE$_2$ levels were measured by enzyme immunoassay. Results are the mean±SEM from 2 different cultures performed in triplicate. *p<0.05, **p<0.01, ***p<0.001 vs. controls. (C) Astrocytes were pretreated with indomethacin (Indo, 0.01 mM) for 15 min, geldanamycin (GA, 1 μM) for 30 min, or buthionine sulfoximine (BSO, 100 μM) for 24 h before treatment with 10 μM MeHg for 3 h. The figure represents a composite of multiple experiments; PGE$_2$ in each treatment group is expressed as the ratio to its intra-study control (cont). The effects of COX inhibition and GSH depletion were assessed in 3 different astrocyte cultures performed in triplicate; the effect of Hsp90 antagonism with GA was determined in 2 different cultures performed in triplicates. *p<0.01 vs. control; # p<0.05, ###<0.001 vs. MeHg treatment.
doi:10.1371/journal.pone.0098161.g002

MeHg alters the association between Hsp90 and neuronal nNOS and iNOS

Given the observation that MeHg increases the association between Hsp90 and PGES/p23, we were interested in whether MeHg influences other Hsp90-client protein interactions, particularly with nNOS. Astrocytes were activated with LPS (1 μg/ml) and IFNγ (100 u/ml) for 18–24 h before treatment with 10 μM MeHg for 1 h. LPS/IFNγ increased both nNOS and iNOS expression (Figure 4 A and B). MeHg treatment increased nNOS expression after LPS/IFNγ stimulation (Figure 4A), but did not change iNOS expression (Figure 4B), suggesting that nNOS is more responsive to MeHg. We next examined whether MeHg
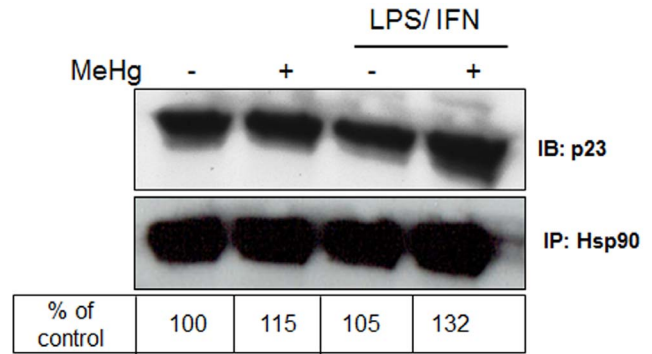

Figure 3. Interaction of Hsp90 and PGES/p23 is promoted by MeHg. Hsp90 was immunoprecipitated from whole cell extracts of astrocytes treated for 1 h with 10 μM MeHg, 18 h with LPS (1 μμg/ml)/IFNγ (100 u/ml), or both 18 h LPS/INFγ and 1 h MeHg. Equal amounts of immunoprecipitated Hsp90 was used for immunoblotting of PGES/p23. Blot is representative of three separate experiments. Percent change in the amount of p23 relative to Hsp90 is shown below the blot, where basal levels of the interaction are designated 100% and increases in the interaction are values above 100.
doi:10.1371/journal.pone.0098161.g003

affected Hsp90 binding to nNOS. nNOS was immunoprecipitated from protein lysates of astrocytes treated with LPS (1 μg/ml) and IFNγ (100 u/ml) for 18 h before treatment with 10 μM MeHg for 6 h, and Hsp90 was immunoblotted. Hsp90 and nNOS co-immunoprecipitate in the presence of LPS/IFNg, and this binding complex was increased following MeHg exposure (Figure 4C).

MeHg uncouples NOS activity and increases NOS-derived superoxide (•O$_2^-$) production

Since association of Hsp90 with nNOS enhances nNOS activity [37], we next determined whether there was increased NO signaling immediately following MeHg treatment. Release of NO was assessed in astrocytes treated with 10 μM MeHg for 30 min and then loaded with 20 μM 4,5-diaminofluorescein diacetate (DAF2DA). Fluorescent images were taken 20 min following addition of the DAF2DA. Astrocytes treated with MeHg showed significantly higher levels of NO than control cells (Figure 5A). NO activates guanylate cyclase to produce cGMP as a second messenger in various cell signaling pathways. Therefore, we quantified cGMP levels in astrocytes treated with 10 μM MeHg for 1 h using an enzyme immunoassay. cGMP levels were reduced by ~50% in astrocytes treated with MeHg relative to controls (Figure 5B). An increase in NO released by the cells but a dampening of the NO-dependent second messenger, cGMP, suggests that MeHg uncouples NO release from downstream NO-dependent signaling.

Under conditions of substrate depletion and certain pathological conditions, such as hypertension and atherosclerosis, nNOS has been shown to produce ROS, particularly H$_2$O$_2$ and •O$_2^-$ [38,39]. •O$_2^-$ production was assessed by confocal microscopy of hydroethidium-loaded astrocytes exposed to 10 μM MeHg for 20 min. MeHg significantly increased the amount of ethidium fluorescence (Figure 6A). H$_2$O$_2$ is formed from •O$_2^-$ in the presence of superoxide dismutase and catalase. To examine H$_2$O$_2$ formation, we preloaded astrocytes with 50 μM 2',7'-dichlorodihydrofluorescein for 30 min and then treated with 5, 10, and 20 μM MeHg for 1 h. DCF fluorescence was significantly increased in astrocytes treated with 10 and 20 μM MeHg as compared to control (Figure 6B). Together, these data demonstrate that MeHg increases several ROS produced in astrocytes,
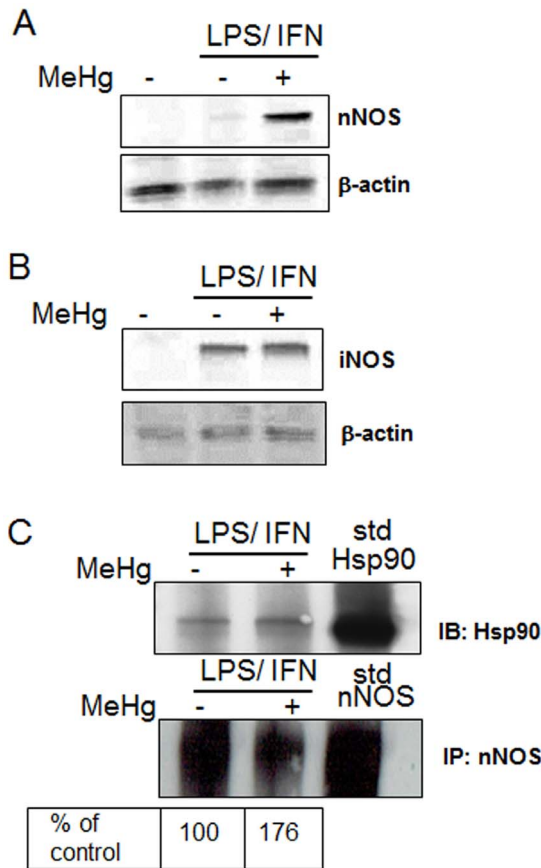
Figure 4. MeHg increases nNOS and iNOS levels. Astrocytes were treated with LPS (1 μg/ml)/IFNγ (100 u/ml) for 18 h and/or 10 μM MeHg for 6 h. Levels of (A) nNOS and (B) iNOS were measured by western blot analysis. (C) nNOS was immunoprecipitated from whole cell extracts of astrocytes stimulated with LPS (1 μg/ml)/IFNγ (100 u/ml) for 18 h alone or followed by 10 μM MeHg for 6 h. Equal amount of immunoprecipitated nNOS was used for immunoblotting of Hsp90. Protein standards for both Hsp90 and nNOS were loaded into the same lane of the gel. Blot is representative of three separate experiments. Percent change in the amount of Hsp90 relative to nNOS is shown below the blot, where basla levels of the interaction are designated 100% and increases in the interaction are values above 100.
doi:10.1371/journal.pone.0098161.g004

including the ROS, NO which can interact $\bullet O_2^-$ to form the highly toxic peroxynitrite $(OONO^-)$ [40].

Discussion

MeHg is a known neurotoxin that has been shown to affect astrocytes as well as neurons, leading to cellular dysfunction and neuronal death. We have previously shown that MeHg induces astrocytic swelling triggering glutamate release and inhibits the uptake of cystine and cysteine [41,42,43,44,45], reducing the astrocytes' ability to synthesize GSH and buffer ROS. Increased glutamate release stimulates N-methyl D-aspartate (NMDA) receptors on neurons increasing intracellular Ca^{2+} concentrations, which leads to the activation of nNOS and mitochondrial dysfunction [46]. MeHg also has been shown to activate cPLA2, possibly through increased Ca^{2+} concentrations, releasing AA, and ultimately leading to protein carbonylation and synthesis of prostaglandins and isoprostanes [33,47]. Central to both prosta-glandin synthesis and nNOS activation pathways is regulation by
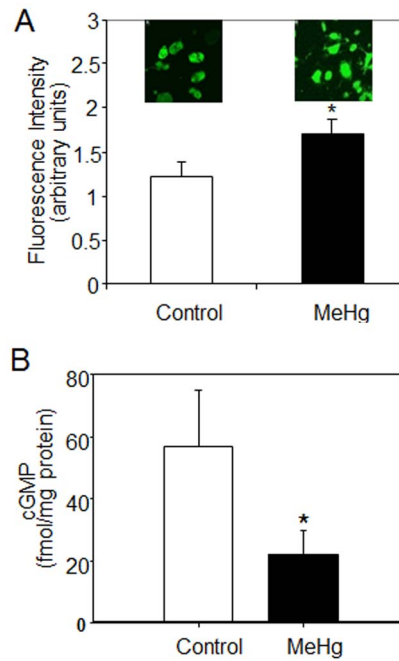

Figure 5. Disruption of NO signaling by MeHg. (A) Astrocytes were treated for 30 min with 10 μM MeHg. After addition of 20 μM DAF2DA, fluorescence images were taken and fluorescence intensity was calculated. Results are mean ± SEM from 3 independent experiments. *p<0.05 vs. control. (B) cGMP concentrations were measured by enzyme immunoassay from astrocytes treated for 1 h with 10 μM MeHg. Results are mean ± SEM from 4–6 separate astrocyte preparations. *p<0.05 vs. control.
doi:10.1371/journal.pone.0098161.g005
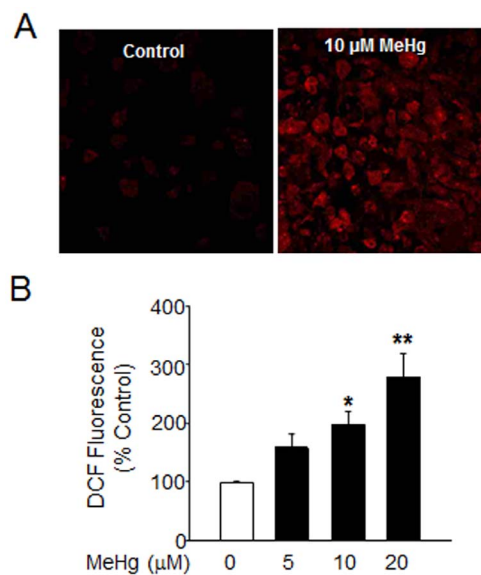
Figure 6. MeHg increases ROS in astrocytes. (A) To assess $\bullet O_2^-$ production, astrocytes were exposed to hydroethidium and then treated with 10 μM MeHg for 20 min. Images are representative of 3 independent experiments. (B) H_2O_2 production was assessed by loading. astrocytes with 50 μM 2′,7′-dichlorodihydrofluorescein for 30 min. Astrocytes were then treated with 5, 10, and 20 μM MeHg for 1 h and DCF fluorescence was measured. Results are depicted as % DCF fluorescence in control astrocytes. Results are mean ± SEM from 4 separate astrocyte preparations. *p<0.05 vs. control.
doi:10.1371/journal.pone.0098161.g006

the Hsp90 chaperone. Our data are the first to describe that MeHg alters Hsp90 chaperone function with subsequent activation of nNOS and PGES/p23, leading to increased release of PGE$_2$ and ROS from astrocytes.

The neuroprotective roles of heat shock chaperone proteins are well recognized. Both Hsp70 and Hsp90 protect neurons from thermal injury, ischemia, protein aggregation, and apoptosis [48,49,50]. Hsp90 can also exert antioxidant effects in glial cells [49,51]. Conversely, Hsp90 has been implicated in neurodegenerative diseases, as it is found in protein aggregates and cellular inclusion bodies in Parkinson's disease (PD) [52]. In certain conditions, Hsp70 and Hsp90 act antagonistically, with Hsp70 affording protection and Hsp90 accelerating damage, such as in polyglutamine-mediated neurodegeneration and amyloid beta toxicity [52]. Congruent with these antagonistic roles, the Hsp90 inhibitor, geldanamycin, induces an overexpression of Hsp70 and protects against 1-methyl-4-phenyl-1,2,3,6-tetrahydropyridine (MPTP)-induced dopaminergic toxicity [53]. Due to these dual roles for Hsp90, and the shared pathways between neurodegenerative diseases and MeHg exposure, we explored whether MeHg activated or inhibited Hsp90. Hsp70 has been shown to be up-regulated in the cerebellum of mice exposed to MeHg, which may represent a protective response [54]. MeHg decreases glutathione peroxidase (GPx) and thioredoxin reductase (TrxR) activities through protein-thiol modification. These modifications often target the proteins for degradation, potentially mediated by Hsp70 chaperone activity. Increased Hsp70 in mouse cerebellum was correlated with decreased GPx1, GPx4, and TrxR1 protein levels [54]. Up-regulation of Hsp70 by MeHg is conserved in nonvertebrates; MeHg treatment increases HSP-4, the nematode homologue to Hsp70, in *Caenorhabditis elegans* [55], highlighting an important conserved response to the metal. We have observed that in primary cultured rat astrocytes that MeHg decreased Hsp90 levels in a concentration- and time-dependent manner (Figure 1). The down regulation of Hsp90 is unique to MeHg treatment as both chick embryos and rats treatment with HgCl$_2$ show increased Hsp90 protein levels [56,57]. These contrasting data suggest that Hsp90 responds differently to inorganic and organic Hg species. In addition to decreasing Hsp90 protein expression, we have shown that MeHg alters Hsp90 activity, as there are critical reactive cysteines found in the vicinity of Hsp90's ATP binding site that are potential targets for MeHg protein adduction and/or MeHg-induced oxidative stress.

PGES/p23 is an important Hsp90 client protein involved in MeHg toxicity. Previously, we have shown that MeHg increases the activity of cPLA2 in both neurons and astrocytes, causing an increase in AA [33,58]. AA is converted into PGH$_2$ by the actions of cyclooxygenases and peroxidase, which is a precursor for both isoprostanes and PGE$_2$. Here we show that astrocytes release PGE$_2$ in response to MeHg, in agreement with previous reports [47]. Depletion of GSH by BSO prevented PGE$_2$ release, suggesting that MeHg-dependent release of PGE$_2$ is redox-dependent. Astrocytes released significantly less PGE$_2$ in response to MeHg when pretreated with the Hsp90 antagonist, GA (Figure 2). GA binds to the ATP binding site on Hsp90, inhibiting its ATP-dependent chaperone function, however GA does not prevent binding of Hsp90 to client proteins or disrupt existing Hsp90/client protein complexes [59]. Indeed, MeHg was shown to increase the interaction between Hsp90 and PGES/p23 in activated and resting astrocytes (Figure 3). Since Hsp90 chaperone function antagonism resulted in decreased PGE$_2$ release following

MeHg exposure, our data suggest that despite the loss of Hsp90 protein expression by MeHg, Hsp90 is capable of forming a complex with its client protein, PGES/p23. Excess PGE$_2$ promotes Ca^{2+}-dependent glutamate release from cultured astrocytes and brain slices, which combined with blocked glutamate reuptake by MeHg-induced AA release, results in markedly increased levels of extracellular glutamate and excitotoxicity [4,60,61].

Activation of the NMDA receptor increases intracellular concentration of Ca^{2+} and activates NOSs, which are also client proteins of Hsp90 [22,62]. As astrocytes express nNOS and iNOS [63,64], we investigated NOS activation as a second measure of the effect of MeHg on Hsp90 client protein binding. MeHg increased levels of both nNOS and iNOS in activated astrocytes, with a greater increase noted for nNOS (Figure 4). Additionally, MeHg increased the protein-protein interaction between nNOS and Hsp90 (Figure 4). The increase in nNOS and iNOS expression was associated with increased NO synthesis in response to MeHg treatment, suggesting that MeHg activates NOS. Additionally, we found that MeHg treatment decreased cGMP levels, the second messenger mediating downstream vasoactive NO signaling (Figure 5). Thus there appears to be an uncoupling of NO release from NO-dependent signaling in the presence of MeHg. Inhibition of the NO-cGMP signaling pathway has been observed in 3-month-old rats exposed to MeHg and polychlorinated biphenols (PCB126 and PCB153), leading to learning deficits (Piedrafita et al., 2008). NO has a number of important biochemical and physiological functions in the CNS, including neurotransmission, learning, regulation of glycolytic enzymes, pain perception, immune function and vascular regulation. Conversely, excessive NO release is cytotoxic. Over activation of glutamate receptors associated with cerebral ischemia and other excitotoxic processes results in massive release of NO [65]. NO mediates cellular toxicity by damaging critical metabolic enzymes and by reacting with $\bullet O_2^-$ to form the even more potent peroxynitrite (ONOO$^-$) [40]. High levels of NO are associated with inflammatory, neurodegenerative and cardiovascular/ischemic pathologies [66]. Several *in vitro* studies show that NO produced by iNOS in astrocytes mediates neuronal cell death after excitotoxic injury [67,68,69]. In our studies, both O_2^- and H_2O_2 were significantly increased following MeHg exposure (Figure 6). Increases in NO and ONOO$^-$ combined with Ca^{2+} overload damages the mitochondrial electron transport chain, resulting in reduced ATP formation, additional $\bullet O_2^-$ formation, and cytochrome *c* release, all of which initiate a damaging cascade leading to neuronal death.

Taken together this study demonstrates for the first time that Hsp90 is an intermediary in MeHg toxicity. While MeHg decreases Hsp90 protein content from astrocytes following prolonged exposure, Hsp90 remains capable of interacting with its client proteins, PGES/p23 and nNOS, which generate increased amounts of PGE$_2$, NO, and ROS in the presence of MeHg. Both of these pathways converge on glutamate signaling, mitochondrial dysfunction, and excitotoxic cell death.

Author Contributions

Conceived and designed the experiments: SC JLA MA. Performed the experiments: SC HZ. Analyzed the data: SC JLA MA. Contributed reagents/materials/analysis tools: HZ. Wrote the paper: SC JLA MA.

References

1. Ekino S, Susa M, Ninomiya T, Imamura K, Kitamura T (2007) Minamata disease revisited: an update on the acute and chronic manifestations of methyl mercury poisoning. Journal of the neurological sciences 262: 131–144.

2. Grandjean P, Satoh H, Murata K, Eto K (2010) Adverse effects of methylmercury: environmental health research implications. Environmental health perspectives 118: 1137–1145.

3. Clarkson TW, Magos L (2006) The toxicology of mercury and its chemical compounds. Critical reviews in toxicology 36: 609–662.

4. Aschner M, Yao CP, Allen JW, Tan KH (2000) Methylmercury alters glutamate transport in astrocytes. Neurochemistry international 37: 199–206.

5. Brookes N (1992) In vitro evidence for the role of glutamate in the CNS toxicity of mercury. Toxicology 76: 245–256.

6. Charleston JS, Body RL, Bolender RP, Mottet NK, Vahter ME, et al. (1996) Changes in the number of astrocytes and microglia in the thalamus of the monkey Macaca fascicularis following long-term subclinical methylmercury exposure. Neurotoxicology 17: 127–138.

7. Garman RH, Weiss B, Evans HL (1975) Alkylmercurial encephalopathy in the monkey (Saimiri sciureus and Macaca arctoides): a histopathologic and autoradiographic study. Acta neuropathologica 32: 61–74.

8. Allen JW, Mutkus LA, Aschner M (2001) Methylmercury-mediated inhibition of 3H-D-aspartate transport in cultured astrocytes is reversed by the antioxidant catalase. Brain research 902: 92–100.

9. Aschner M, Du YL, Gannon M, Kimelberg HK (1993) Methylmercury-induced alterations in excitatory amino acid transport in rat primary astrocyte cultures. Brain research 602: 181–186.

10. Brookes N, Kristt DA (1989) Inhibition of amino acid transport and protein synthesis by HgCl2 and methylmercury in astrocytes: selectivity and reversibility. Journal of neurochemistry 53: 1228–1237.

11. Mullaney KJ, Fehm MN, Vitarella D, Wagoner DE, Jr., Aschner M (1994) The role of -SH groups in methylmercuric chloride-induced D-aspartate and rubidium release from rat primary astrocyte cultures. Brain research 641: 1–9.

12. Rothstein JD, Dykes-Hoberg M, Pardo CA, Bristol LA, Jin L, et al. (1996) Knockout of glutamate transporters reveals a major role for astroglial transport in excitotoxicity and clearance of glutamate. Neuron 16: 675–686.

13. Farina M, Aschner M, Rocha JB (2011) Oxidative stress in MeHg-induced neurotoxicity. Toxicology and applied pharmacology 256: 405–417.

14. Shanker G, Aschner JL, Syversen T, Aschner M (2004) Free radical formation in cerebral cortical astrocytes in culture induced by methylmercury. Brain research Molecular brain research 128: 48–57.

15. Herculano AM, Crespo-Lopez ME, Lima SM, Picanco-Diniz DL, Do Nascimento JL (2006) Methylmercury intoxication activates nitric oxide synthase in chick retinal cell culture. Brazilian journal of medical and biological research = Revista brasileira de pesquisas medicas e biologicas/Sociedade Brasileira de Biofisica [et al] 39: 415–418.

16. Ikeda M, Komachi H, Sato I, Himi T, Yuasa T, et al. (1999) Induction of neuronal nitric oxide synthase by methylmercury in the cerebellum. Journal of neuroscience research 55: 352–356.

17. Mori N, Yasutake A, Hirayama K (2007) Comparative study of activities in reactive oxygen species production/defense system in mitochondria of rat brain and liver, and their susceptibility to methylmercury toxicity. Archives of toxicology 81: 769–776.

18. Carvalho CM, Chew EH, Hashemy SI, Lu J, Holmgren A (2008) Inhibition of the human thioredoxin system. A molecular mechanism of mercury toxicity. The Journal of biological chemistry 283: 11913–11923.

19. Farina M, Campos F, Vendrell I, Berenguer J, Barzi M, et al. (2009) Probucol increases glutathione peroxidase-1 activity and displays long-lasting protection against methylmercury toxicity in cerebellar granule cells. Toxicological sciences: an official journal of the Society of Toxicology 112: 416–426.

20. Caplan AJ (1999) Hsp90's secrets unfold: new insights from structural and functional studies. Trends in cell biology 9: 262–268.

21. Taipale M, Jarosz DF, Lindquist S (2010) HSP90 at the hub of protein homeostasis: emerging mechanistic insights. Nature reviews Molecular cell biology 11: 515–528.

22. Bender AT, Silverstein AM, Demady DR, Kanelakis KC, Noguchi S, et al. (1999) Neuronal nitric-oxide synthase is regulated by the Hsp90-based chaperone system in vivo. The Journal of biological chemistry 274: 1472–1478.

23. Pratt WB, Morishima Y, Osawa Y (2008) The Hsp90 chaperone machinery regulates signaling by modulating ligand binding clefts. The Journal of biological chemistry 283: 22885–22889.

24. Segnitz B, Gehring U (1997) The function of steroid hormone receptors is inhibited by the hsp90-specific compound geldanamycin. The Journal of biological chemistry 272: 18694–18701.

25. Tanioka T, Nakatani Y, Kobayashi T, Tsujimoto M, Oh-ishi S, et al. (2003) Regulation of cytosolic prostaglandin E2 synthase by 90-kDa heat shock protein. Biochemical and biophysical research communications 303: 1018–1023.

26. Nardai G, Sass B, Eber J, Orosz G, Csermely P (2000) Reactive cysteines of the 90-kDa heat shock protein, Hsp90. Archives of biochemistry and biophysics 384: 59–67.

27. Beck R, Dejeans N, Glorieux C, Creton M, Delaive E, et al. (2012) Hsp90 is cleaved by reactive oxygen species at a highly conserved N-terminal amino acid motif. PloS one 7: e40795.

28. Beck R, Verrax J, Gonze T, Zappone M, Pedrosa RC, et al. (2009) Hsp90 cleavage by an oxidative stress leads to its client proteins degradation and cancer cell death. Biochemical pharmacology 77: 375–383.

29. Ni M, Aschner M (2010) Neonatal rat primary microglia: isolation, culturing, and selected applications. Curr Protoc Toxicol Chapter 12: Unit 12 17.

30. Ni M, Li X, Yin Z, Sidoryk-Wegrzynowicz M, Jiang H, et al. (2011) Comparative study on the response of rat primary astrocytes and microglia to methylmercury toxicity. Glia 59: 810–820.

31. Morken TS, Sonnewald U, Aschner M, Syversen T (2005) Effects of methylmercury on primary brain cells in mono- and co-culture. Toxicological sciences: an official journal of the Society of Toxicology 87: 169–175.

32. Shanker G, Aschner M (2003) Methylmercury-induced reactive oxygen species formation in neonatal cerebral astrocytic cultures is attenuated by antioxidants. Brain research Molecular brain research 110: 85–91.

33. Shanker G, Mutkus LA, Walker SJ, Aschner M (2002) Methylmercury enhances arachidonic acid release and cytosolic phospholipase A2 expression in primary cultures of neonatal astrocytes. Brain research Molecular brain research 106: 1–11.

34. Tanioka T, Nakatani Y, Semmyo N, Murakami M, Kudo I (2000) Molecular identification of cytosolic prostaglandin E2 synthase that is functionally coupled with cyclooxygenase-1 in immediate prostaglandin E2 biosynthesis. J Biol Chem 275: 32775–32782.

35. Brahmachari S, Fung YK, Pahan K (2006) Induction of glial fibrillary acidic protein expression in astrocytes by nitric oxide. The Journal of neuroscience: the official journal of the Society for Neuroscience 26: 4930–4939.

36. Tani M, Glabinski AR, Tuohy VK, Stoler MH, Estes ML, et al. (1996) In situ hybridization analysis of glial fibrillary acidic protein mRNA reveals evidence of biphasic astrocyte activation during acute experimental autoimmune encephalomyelitis. The American journal of pathology 148: 889–896.

37. Song Y, Zweier JL, Xia Y (2001) Heat-shock protein 90 augments neuronal nitric oxide synthase activity by enhancing Ca2+/calmodulin binding. The Biochemical journal 355: 357–360.

38. Sullivan JC, Pollock JS (2006) Coupled and uncoupled NOS: separate but equal? Uncoupled NOS in endothelial cells is a critical pathway for intracellular signaling. Circulation research 98: 717–719.

39. Xia Y (2007) Superoxide generation from nitric oxide synthases. Antioxidants & redox signaling 9: 1773–1778.

40. Heales SJ, Bolanos JP, Stewart VC, Brookes PS, Land JM, et al. (1999) Nitric oxide, mitochondria and neurological disease. Biochimica et biophysica acta 1410: 215–228.

41. Aschner M, Eberle NB, Miller K, Kimelberg HK (1990) Interactions of methylmercury with rat primary astrocyte cultures: inhibition of rubidium and glutamate uptake and induction of swelling. Brain Res 530: 245–250.

42. Aschner M, Vitarella D, Allen JW, Conklin DR, Cowan KS (1998) Methylmercury-induced inhibition of regulatory volume decrease in astrocytes: characterization of osmoregulator efflux and its reversal by amiloride. Brain Res 811: 133–142.

43. Aschner M, Yao CP, Allen JW, Tan KH (2000) Methylmercury alters glutamate transport in astrocytes. Neurochem Int 37: 199–206.

44. Mutkus L, Aschner JL, Syversen T, Aschner M (2005) Methylmercury alters the in vitro uptake of glutamate in GLAST- and GLT-1-transfected mutant CHO-K1 cells. Biol Trace Elem Res 107: 231–245.

45. Shanker G, Aschner M (2001) Identification and characterization of uptake systems for cystine and cysteine in cultured astrocytes and neurons: evidence for methylmercury-targeted disruption of astrocyte transport. J Neurosci Res 66: 998–1002.

46. Horn TF, Wolf G, Duffy S, Weiss S, Keilhoff G, et al. (2002) Nitric oxide promotes intracellular calcium release from mitochondria in striatal neurons. FASEB journal: official publication of the Federation of American Societies for Experimental Biology 16: 1611–1622.

47. Wormser U, Brodsky B, Milatovic D, Finkelstein Y, Farina M, et al. (2012) Protective effect of a novel peptide against methylmercury-induced toxicity in rat primary astrocytes. Neurotoxicology 33: 763–768.

48. Giffard RG, Xu L, Zhao H, Carrico W, Ouyang Y, et al. (2004) Chaperones, protein aggregation, and brain protection from hypoxic/ischemic injury. The Journal of experimental biology 207: 3213–3220.

49. Lee MW, Park SC, Chae HS, Bach JH, Lee HJ, et al. (2001) The protective role of HSP90 against 3-hydroxykynurenine-induced neuronal apoptosis. Biochemical and biophysical research communications 284: 261–267.

50. Mailhos C, Howard MK, Latchman DS (1994) Heat shock proteins hsp90 and hsp70 protect neuronal cells from thermal stress but not from programmed cell death. Journal of neurochemistry 63: 1787–1795.

51. Jeon GS, Park SW, Kim DW, Seo JH, Cho J, et al. (2004) Glial expression of the 90-kDa heat shock protein (HSP90) and the 94-kDa glucose-regulated protein (GRP94) following an excitotoxic lesion in the mouse hippocampus. Glia 48: 250–258.

52. Luo W, Sun W, Taldone T, Rodina A, Chiosis G (2010) Heat shock protein 90 in neurodegenerative diseases. Molecular neurodegeneration 5: 24.

53. Shen HY, He JC, Wang Y, Huang QY, Chen JF (2005) Geldanamycin induces heat shock protein 70 and protects against MPTP-induced dopaminergic neurotoxicity in mice. The Journal of biological chemistry 280: 39962–39969.

54. Zemolin AP, Meinerz DF, de Paula MT, Mariano DO, Rocha JB, et al. (2012) Evidences for a role of glutathione peroxidase 4 (GPx4) in methylmercury induced neurotoxicity in vivo. Toxicology 302: 60–67.

55. Helmcke KJ, Aschner M (2010) Hormetic effect of methylmercury on Caenorhabditis elegans. Toxicology and applied pharmacology 248: 156–164.

56. Goering PL, Fisher BR, Noren BT, Papaconstantinou A, Rojko JL, et al. (2000) Mercury induces regional and cell-specific stress protein expression in rat kidney. Toxicological sciences: an official journal of the Society of Toxicology 53: 447–457.

57. Papaconstantinou AD, Brown KM, Noren BT, McAlister T, Fisher BR, et al. (2003) Mercury, cadmium, and arsenite enhance heat shock protein synthesis in chick embryos prior to embryotoxicity. Birth defects research Part B, Developmental and reproductive toxicology 68: 456–464.

58. Shanker G, Hampson RE, Aschner M (2004) Methylmercury stimulates arachidonic acid release and cytosolic phospholipase A2 expression in primary neuronal cultures. Neurotoxicology 25: 399–406.

59. Panaretou B, Prodromou C, Roe SM, O'Brien R, Ladbury JE, et al. (1998) ATP binding and hydrolysis are essential to the function of the Hsp90 molecular chaperone in vivo. The EMBO journal 17: 4829–4836.

60. Bezzi P, Carmignoto G, Pasti L, Vesce S, Rossi D, et al. (1998) Prostaglandins stimulate calcium-dependent glutamate release in astrocytes. Nature 391: 281–285.

61. Yu AC, Chan PH, Fishman RA (1987) Arachidonic acid inhibits uptake of glutamate and glutamine but not of GABA in cultured cerebellar granule cells. Journal of neuroscience research 17: 424–427.

62. Rameau GA, Chiu LY, Ziff EB (2003) NMDA receptor regulation of nNOS phosphorylation and induction of neuron death. Neurobiology of aging 24: 1123–1133.

63. Lee MC, Ting KK, Adams S, Brew BJ, Chung R, et al. (2010) Characterisation of the expression of NMDA receptors in human astrocytes. PloS one 5: e14123.

64. Yao SY, Ljunggren-Rose A, Chandramohan N, Whetsell WO, Jr., Sriram S (2010) In vitro and in vivo induction and activation of nNOS by LPS in oligodendrocytes. Journal of neuroimmunology 229: 146–156.

65. Bredt DS, Snyder SH (1994) Nitric oxide: a physiologic messenger molecule. Annual review of biochemistry 63: 175–195.

66. Pacher P, Beckman JS, Liaudet L (2007) Nitric oxide and peroxynitrite in health and disease. Physiological reviews 87: 315–424.

67. Bolanos JP, Heales SJ, Land JM, Clark JB (1995) Effect of peroxynitrite on the mitochondrial respiratory chain: differential susceptibility of neurones and astrocytes in primary culture. Journal of neurochemistry 64: 1965–1972.

68. Golde S, Chandran S, Brown GC, Compston A (2002) Different pathways for iNOS-mediated toxicity in vitro dependent on neuronal maturation and NMDA receptor expression. Journal of neurochemistry 82: 269–282.

69. Lecanu L, Verrecchia C, Margaill I, Boulu RG, Plotkine M (1998) iNOS contribution to the NMDA-induced excitotoxic lesion in the rat striatum. British journal of pharmacology 125: 584–590.